

THE OFFICIAL MAGAZINE OF THE OCEANOGRAPHY SOCIETY

Oceanography

CITATION

Dziak, R.P., S.R. Hammond, and C.G. Fox. 2011. A 20-year hydroacoustic time series of seismic and volcanic events in the Northeast Pacific Ocean. *Oceanography* 24(3):280–293, <http://dx.doi.org/10.5670/oceanog.2011.79>.

COPYRIGHT

This article has been published in *Oceanography*, Volume 24, Number 3, a quarterly journal of The Oceanography Society. Copyright 2011 by The Oceanography Society. All rights reserved.

USAGE

Permission is granted to copy this article for use in teaching and research. Republication, systematic reproduction, or collective redistribution of any portion of this article by photocopy machine, reposting, or other means is permitted only with the approval of The Oceanography Society. Send all correspondence to: info@tos.org or The Oceanography Society, PO Box 1931, Rockville, MD 20849-1931, USA.

A 20-YEAR HYDROACOUSTIC TIME SERIES OF SEISMIC AND VOLCANIC EVENTS IN THE NORTHEAST PACIFIC OCEAN

BY ROBERT P. DZIAK, STEPHEN R. HAMMOND, AND CHRISTOPHER G. FOX



Photos courtesy of Joseph A. Resing

ABSTRACT. For the last 20 years, civilian researchers have used the Sound Surveillance System (SOSUS), a US Navy hydrophone array deployed for anti-submarine warfare during the Cold War, to detect seismic and volcanic activity in the Northeast Pacific Ocean. A total of 46,498 earthquakes have been located along oceanic plate boundaries, providing a comprehensive view of volcano-tectonic activity in the region. During the 20-year interval, the Northeast Pacific spreading centers exhibited both high levels of continued background seismicity (Explorer and Gorda segments) and long periods of quiescence punctuated by brief periods (days to weeks) of intense (> 1000 events/day) earthquake activity. The Juan de Fuca Ridge south of the Cobb Offset is largely aseismic, with the exception of events associated with two three-week-long volcanic eruptions and frequent seismicity at 46°50'N. In contrast, the Endeavour, Explorer, and Gorda Ridges, and the Cobb Offset are highly seismic, producing continuous earthquake activity. Of the seven major episodes of seafloor spreading identified by analysis of the SOSUS data, three resulted in lava eruptions onto the seafloor and release of large hydrothermal plumes. The Blanco Transform produces the most earthquakes and the largest seismic energy release of any Northeast Pacific plate boundary. The Explorer and Gorda plates are also very seismically active, which is consistent with these areas being highly fractured deformation zones that are structurally independent from the Juan de Fuca plate.

INTRODUCTION

Following the end of the Cold War in the late 1980s, the US Navy sought environmental applications for many of its military assets and developed a dual-use program to share technology with civilian research groups (Fox and Hammond, 1994). At this same time, the National Oceanic and Atmospheric Administration (NOAA) Vents Program was actively investigating volcanic and hydrothermal processes along Northeast Pacific Ocean spreading centers. Based on the previous success of civilian researchers during the 1960s using the Navy's Sound Surveillance System (SOSUS) and the Air Force's Missile Impact Location System hydrophones to detect otherwise unobserved seafloor volcanic activity (Johnson et al., 1963), the Vents Program established a partnership with the Navy to once again access SOSUS low-frequency hydrophone data (Fox and Hammond, 1994). The

US Navy began installation of the SOSUS system in the mid-1950s for use in anti-submarine warfare. SOSUS consists of bottom-mounted hydrophone arrays connected by undersea communication cables to facilities onshore. The individual arrays are installed primarily on continental slopes and seamounts at locations optimized for undistorted long-range acoustic propagation. Their position within the oceanic sound channel and the sensitivity of these large-aperture arrays allows the system to detect radiated power of less than a watt at ranges of several hundred kilometers. Several key SOSUS arrays lie within 500 km of the Northeast Pacific spreading centers.

The joint NOAA/Oregon State University (OSU) hydroacoustic research program has used SOSUS since 1991 to detect earthquake-generated Tertiary (*T*-) Phases (Tolstoy and Ewing, 1950), which propagate efficiently within the ocean's low-velocity waveguide. These

data can provide significant improvements in the location and detection capability afforded by land-based seismic stations, improving the completeness level of detection by 1.5–2.0 orders of magnitude for the remote areas of the ridge crest (Bohnenstiehl et al., 2002). The scientific contributions of hydroacoustic studies have been numerous. For example, they have revolutionized our understanding of mid-ocean ridge eruptive processes (e.g., Fox et al., 1995; Dziak and Fox, 1999), illuminated the impact of submarine earthquakes on hydrothermal systems (e.g., Johnson et al., 2000; Dziak et al., 2003), addressed a wide variety of tectonic problems (e.g., Smith et al., 2002; Bohnenstiehl et al., 2002, 2004; Dziak, 2006), and recently demonstrated the predictability of earthquakes on oceanic transform faults (McGuire et al., 2005). Because the Navy does not archive the SOSUS records, the near continuous 20-year library of North Pacific SOSUS digital data collected by NOAA/OSU represents a globally unique earthquake and ocean acoustic data set.

Tectonic Setting and General Patterns of Northeast Pacific Earthquakes

The SOSUS earthquake data set provides valuable insights into the long-term seismic activity of Northeast Pacific Ocean plate boundaries. The relatively small Juan de Fuca (JdF) plate (Figure 1, inset) is a remnant of the Farallon plate. It is bounded by a transform margin with the much larger Pacific plate and is being subducted beneath North America along the Cascadia subduction zone, which lies along its eastern margin. The Pacific and North American plates also impart

a northeast-southwest compressional stress regime throughout the JdF plate (Wang et al., 1997). Consistent with this tectonic setting, the JdF plate exhibits highly seismic ridge segments and transform boundaries and high rates of intraplate seismicity along its northern and southern edges. High deformation rates at the edges of the JdF plate are presumably due to the subduction resistance of relatively young plates. The northern deformation zone of the JdF plate is referred to as the Explorer plate. The JdF and Explorer plates are separated by the Nootka Fault (Riddihough, 1984). The southern deformation zone is referred to as the Gorda plate, separated from the JdF by the Blanco Fracture Zone (Wilson, 1989). Hereafter, when we reference the JdF plate, this designation includes the northern and southern deformation zones unless otherwise noted.

The full 20-year SOSUS event catalog (Figure 1) shows that the Blanco Transform, the Sovanco Transform, the northern Juan de Fuca Ridge, and the Explorer and Gorda plates exhibit high levels of earthquake activity. These plate boundaries are by far the largest source of seismic energy release in the Northeast Pacific. In marked contrast, for this period of monitoring, the Juan de Fuca Ridge (from the Cobb Offset to the Blanco Transform) and the interior of the JdF plate were essentially aseismic, with only a few notable earthquake swarms providing the rare exceptions.

Unique Tectonic and Volcanic Questions in the Northeast Pacific

SOSUS data provide insights and complementary information relevant to a variety of geoscience issues in the Northeast Pacific Ocean. Most notably, the Cascadia subduction zone is a seismically enigmatic boundary because, despite apparently generating great megathrust earthquakes ($M > 9$) at 600–1,000 year intervals (Goldfinger et al., 2003), there have been very few small- to moderate-sized earthquakes detected at the interplate interface since comprehensive global seismic monitoring began in the early 1960s. The SOSUS network also shows the Cascadia subduction zone is essentially aseismic, with only a few isolated earthquakes occurring over the 20-year recording period. This lack of seismicity may be due to the interplate interface currently being “locked,” with little slip during the intraseismic interval between great earthquakes (Heaton and Hartzell, 1987), although slip on the deeper interface occurs via cycles of slow slip and tremor-like (non-earthquake) seismic events (Rogers and Dragert, 2003).

In 1996, the New Millennium Observatory was established at Axial Volcano to study, in situ, volcanic events and the perturbations they cause to hydrothermal and biological environments and processes (Embley and Baker, 1999). Axial Volcano is a hotspot volcano that overlies the central segment

of the Juan de Fuca Ridge at the intersection with the Cobb-Eikelberg hotspot chain. Due to its relatively robust magma supply, the volcano rises some 800 m above the adjacent ridge. Axial Volcano erupted in 1998, and SOSUS detected and located the seismicity associated with the lava eruption at the summit (and the subsequent magma dike intrusion 60 km down-rift; Dziak and Fox, 1999). This eruption was the first seafloor eruption detected remotely and monitored by in situ instruments (Embley et al., 1999). However, Axial Volcano has remained essentially aseismic to the SOSUS detection level since the 1998 eruption, implying this eruption episode significantly reduced levels of crustal stress within the volcano’s caldera and adjacent rift zones. Recent ocean bottom hydrophone deployments and bottom pressure recordings since the last eruption show a steadily increasing rate of microseismicity ($1,000 \text{ events yr}^{-1}$; Haxel et al., 2010) and inflation of the caldera floor at a rate of about 50 cm yr^{-1} , consistent with magmatic resupply of the volcano and providing the basis for the forecast of the next eruption in ~ 2020 (Nooner and Chadwick, 2009). Because of this established history of eruptive activity and indications that another eruption is likely in the near future, Axial Volcano was selected as a primary instrumented node site for the National Science Foundation-sponsored Regional Cabled Observatory (OOI, 2006).

Robert P. Dziak (robert.p.dziak@noaa.gov) is Professor, Cooperative Institute for Marine Resources Studies/Oregon State University, Hatfield Marine Science Center, Newport, OR, USA. **Stephen R. Hammond** is Leader, National Oceanic and Atmospheric Administration (NOAA)/Pacific Marine Environmental Laboratory Ocean Environment Research Division, Newport, OR, USA. **Christopher G. Fox** is Director, NOAA/National Geophysical Data Center, Boulder, CO, USA.

HYDROACOUSTIC METHODS

The map presented in Figure 1 shows the hydroacoustic *T*-Phase locations (hereafter referred to as *T*-waves) derived for the Northeast Pacific Ocean seismic events detected by SOSUS.

Typically, a submarine earthquake will produce seismic waves that propagate through the shallow oceanic crust and convert to an acoustic *T*-wave at the seafloor-ocean interface. Because acoustic *T*-waves propagate laterally in the ocean sound channel, they obey cylindrical spreading (r^{-1}) energy loss as opposed to the spherical spreading (r^{-2}) of solid Earth seismic *P*- and *S*-waves. Consequently, sound channel hydrophones can often detect smaller ($m_b > 2.5$) and therefore more numerous earthquakes than land-based seismic networks (Dziak et al., 2004).

The SOSUS hydrophone arrays are placed at fixed locations on the seafloor, and therefore the area of optimal coverage for the system is predetermined. Fortunately, the SOSUS geometry is well positioned for excellent monitoring of the North Pacific spreading systems. An iterative gradient-expansion (Marquardt) algorithm, which minimizes the difference between the observed and predicted arrival time at each hydrophone, is used to estimate the source location and origin time.

T-wave travel times are computed from the sound velocity along a path derived from oceanic sound speeds (Teague et al., 1990). After determining the location of an event, independent estimates of the acoustic source level are calculated at each hydrophone by correcting the received sound intensity levels by a transmission loss factor that accounts for spherical spreading into the sound channel and cylindrical spreading along the propagation path. The mean of these source levels provides a first-order estimate of earthquake size that has been used to statistically assess the completeness level of *T*-wave catalogs

in the Pacific and Atlantic Oceans. It is estimated that use of omni-directional hydrophones results in a detection threshold of $\sim 2.5 m_b$ (Bohnenstiehl et al., 2002), much lower than the Pacific Northwest land-based seismic network detection threshold of $\sim 4.0 m_b$ (Braunmiller and Nabelek, 2008).

The number and location of SOSUS stations available to derive Northeast

Pacific earthquake locations has varied during the 20 years of this study. From 1991 to 1995, the NOAA/OSU group relied solely on hydrophone arrays along the coast to locate Northeast Pacific earthquakes. In 1995, the number of arrays expanded considerably to include arrays located in the Central, North, and West Pacific. These additional arrays significantly improved location accuracy

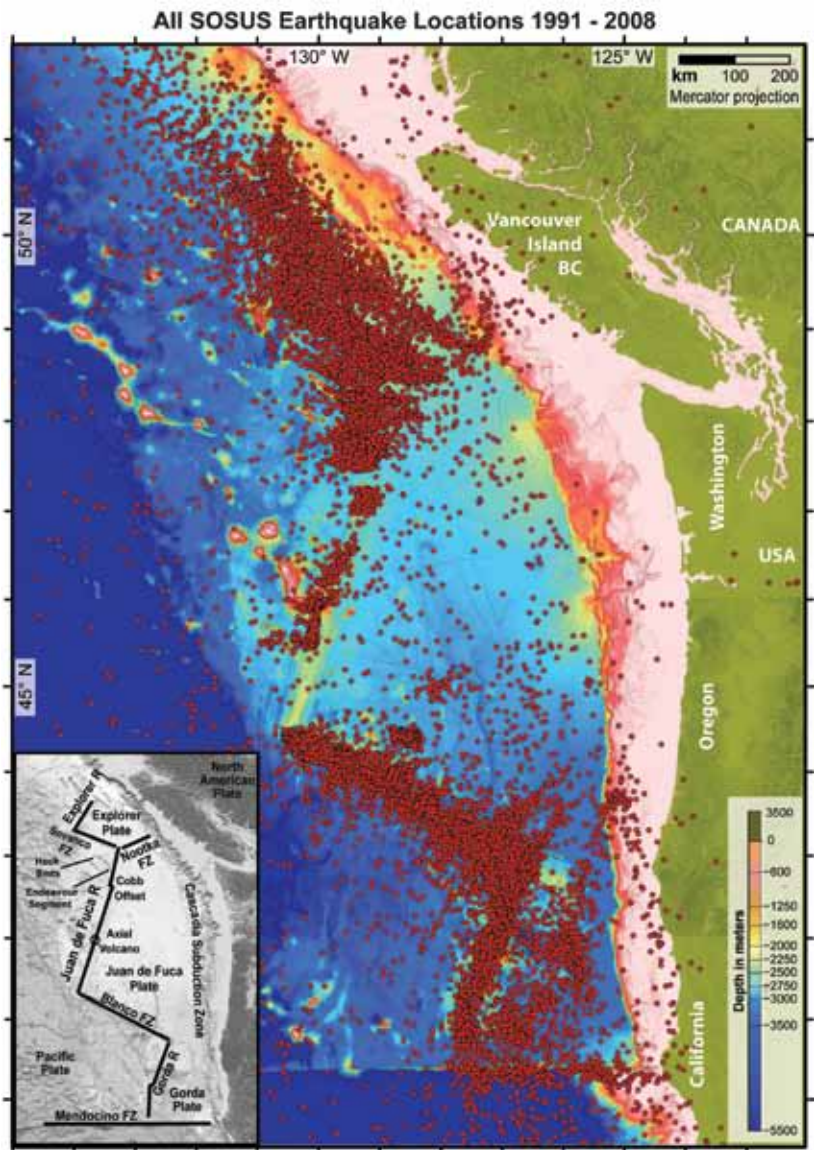


Figure 1. Northeast Pacific Ocean earthquake locations (red dots) derived using the US Navy SOSUS-NOAA hydroacoustic monitoring system from September 1991 through January 2011. A total of 47,934 events were located using > 3 hydrophone stations from throughout the northeastern Pacific.

by providing better azimuthal distribution of recording stations relative to the Northeast Pacific plate boundaries, thus reducing error when estimating an event's latitude and longitude. Since 2000, several arrays were intermittently offline for long periods of time, resulting in gaps in the SOSUS earthquake database. This has again been the situation since 2008 when critical coastal arrays have been unavailable, and although archiving of SOSUS hydrophone data has been ongoing to date (June 2011), comprehensive regional locations for the Northeast Pacific have been estimated only through July 2008. Central and West Pacific hydrophones are currently available, however, allowing detection

and location of large earthquake swarms (both in magnitude and number) on a case-by-case basis.

HYDROACOUSTIC EARTHQUAKE LOCATIONS AND ERROR

Although the regression algorithm used to derive *T*-wave earthquake locations does calculate a covariance matrix that provides an error ellipse for derived earthquake locations, the low number of azimuthally independent hydrophone stations available (≤ 10) does not allow for exceptionally well-constrained estimates of location error. To assess the geometry of the SOSUS array and gauge the variation in location error,

an indirect method based on standard Monte Carlo simulation techniques with calibrations based on known sound sources is applied to the SOSUS array (Figure 2; Fox et al., 2001). The error analysis was repeated for a large grid of reference points (at 0.25° intervals), providing the error surface for each parameter (latitude, longitude, and origin time) over the entire Northeast Pacific study area (Figure 2). The model uses all available SOSUS hydrophone arrays, and thus represents an optimal location error, given that arrays have gone offline at various times. Estimated errors range from 0.5–3.5 km in latitude and 0.8–2 km in longitude along the Explorer, Juan de Fuca, and Gorda Ridges and their associated transform faults (at the 68% confidence interval). These modeled location errors are similar to those obtained from previous simulations of SOSUS and other hydroacoustic arrays (Slack et al., 1999; Fox et al., 2001).

In general, there is no significant systematic variation of uncertainty, although events with the highest uncertainty tend to lie at the northern or southern boundaries of the study region where hydrophone geometry is not as ideal as near the middle latitudes. The accuracy of *T*-wave-determined epicenters has in the past been verified by the successful observation of active seafloor volcanism by field expeditions directed to the *T*-wave source location (e.g., Fox et al., 1995; Dziak and Fox, 1999). Because the location simulation assumes a point source, while the actual region of *T*-wave generation may encompass several square kilometers of seafloor (Slack et al., 1999), the simulated error field is perhaps best interpreted through

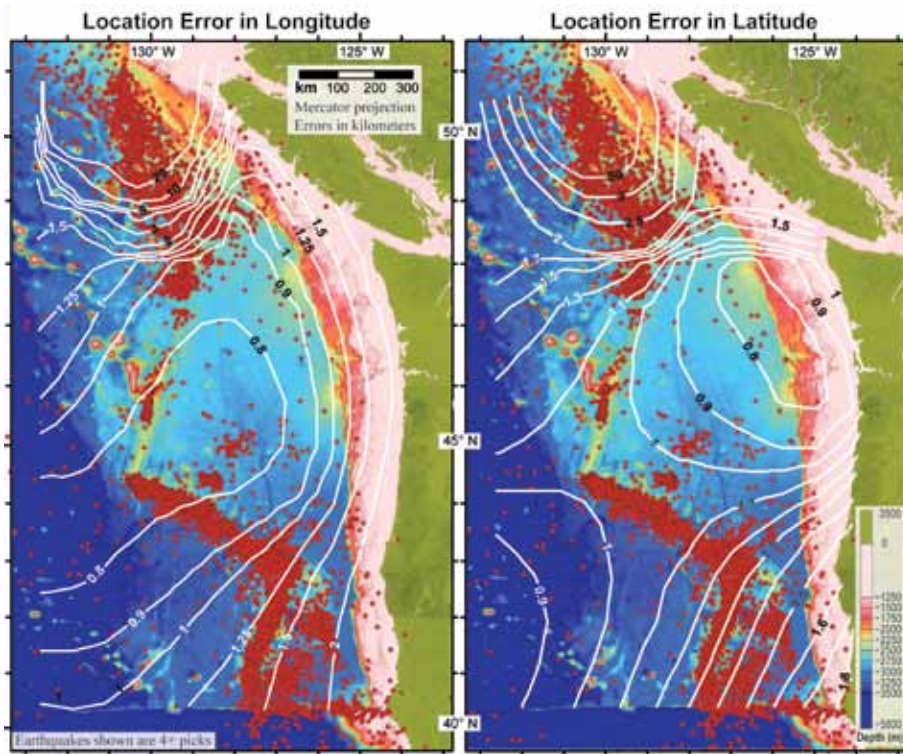


Figure 2. Simulated location errors (in km at the 68% confidence limit) in longitude (left) and latitude (right) for the SOSUS array in the Northeast Pacific. A normally distributed 0.5 sec pick error has been introduced to all arrivals at six omni-directional hydrophones. There are 100 simulations at each 0.25-degree node. Earthquakes located from 1991 to 2011 using ≥ 4 SOSUS hydrophones (red dots) are shown relative to predicted location errors. Predicted origin time errors (not shown) range from 0.3 to 1 sec within the array. Bathymetry is from Sandwell and Smith (1997) satellite altimetry.

such relative comparisons. Overall, the SOSUS-derived earthquake locations are consistently positioned along the active Northeast Pacific plate boundaries. By comparison, the locations for ocean earthquakes derived using land-based seismic networks (National Earthquake Information Center online catalog) are typically tens of kilometers north and east of the JdF plate boundaries (Figure 3). This discrepancy is likely due to inaccurate seismic velocity models and azimuthally limited seismic station locations (Braunmiller and Nabelek, 2008).

Overall, the western Blanco Transform Fault, the Juan de Fuca Ridge south of the Cobb Offset, and the central JdF plate are areas with the best earthquake location accuracy/lowest uncertainty. The eastern Blanco Transform, Gorda Ridge, western Gorda plate, and Endeavour and Middle Valley segments north of the Cobb Offset; the Sovanco Transform; and the Explorer Ridge have higher location uncertainty, but are still within areas of good hydrophone array coverage. Because of the array positions, events associated with the northern Explorer Ridge, the Cascadia subduction zone, the eastern Mendocino Transform, and Queen Charlotte fault areas all have relatively high location uncertainties and low-quality earthquake locations.

Association of SOSUS Seismicity with Ridge, Plate, and Transform Fault Structures

Review of JdF plate seismicity (Figures 1 and 4) permits several intriguing first-order observations. The Northeast Pacific spreading centers can exhibit both high levels of continued, background seismicity (Explorer and Gorda

Ridges) and long periods of quiescence punctuated by brief periods (days to weeks) of intense (> 1000 events/day) earthquake activity. The Juan de Fuca Ridge from the Cobb Offset to the Blanco Transform is largely aseismic. The three exceptions to Juan de Fuca Ridge aseismicity are two brief (two-to-three-week long) seafloor spreading events (the CoAxial segment and Axial Volcano) and the Juan de Fuca Ridge segment at 46°50'N, which has exhibited continuous seismic activity during the 20 years of SOSUS recording. The 46°50'N location is the site of elevated bathymetry on the rift axis, and there is a seamount on the adjacent ridge flank, both indicating there is an upper mantle melt anomaly beneath the ridge crest here. Also, the

Endeavour, Explorer, and Gorda Ridges are highly seismic, and produce essentially continuous earthquake activity. The Gorda Ridge is composed of five structurally independent segments, each with a discrete cluster of earthquake activity that varies systematically through space and time (e.g., Walker and Hammond, 1998). The Cobb Offset and Endeavour segment, however, produce many more earthquakes over the long term than the other Northeast Pacific spreading center segments.

The Blanco and Sovanco Transform Faults exhibit high levels of continuous earthquake activity. The Blanco Transform produces more earthquakes and total seismic energy release than any other Northeast Pacific plate boundary

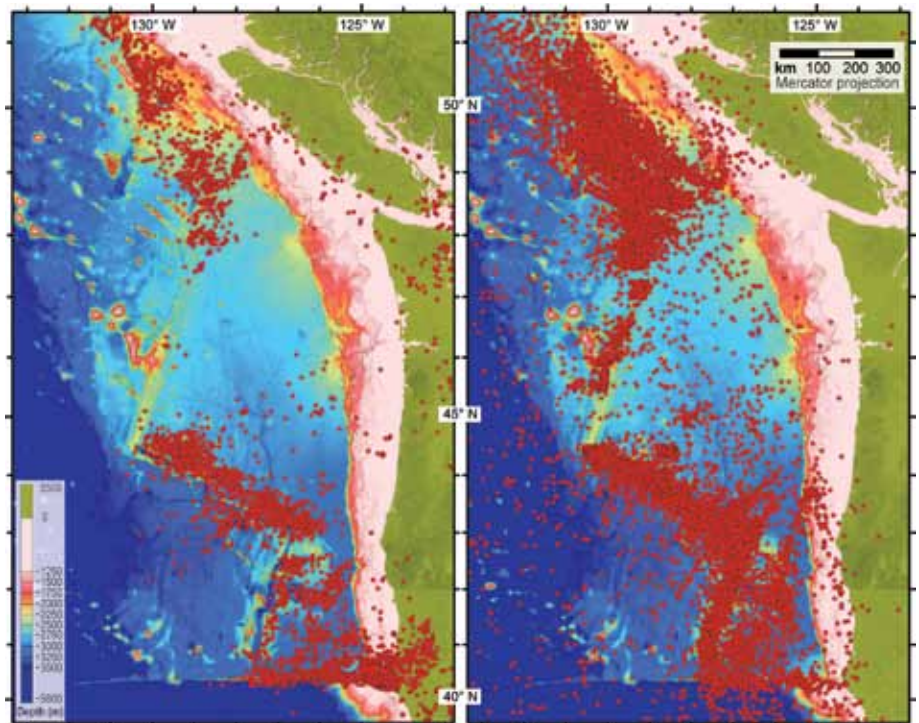


Figure 3. Northeast Pacific earthquake locations from 1991 to 2011 derived from the National Earthquake Information Center (NEIC) online catalog (left) and SOSUS (right). A total of 47,934 earthquakes were located by SOSUS compared to 3,023 earthquakes located from land-based seismic networks. The hydroacoustic earthquake locations are more closely associated with the active Northeast Pacific plate boundaries; the NEIC locations are typically offset to the northeast of the plate boundaries.

(Figure 4). The Blanco Transform has two clear seismic segments, where the western transform ($\sim 44^\circ\text{N}$) has exhibited an order of magnitude more earthquakes than the eastern transform ($\sim 43^\circ\text{N}$). The eastern segment is the most consistent producer of the largest earthquakes in the region, with five $M_w > 6$ earthquakes since 1991 (Boettcher and McGuire, 2009). The nearly constant seismic activity on the Blanco Transform is likely attributable to continued, relatively rapid JdF plate motion and convergence at the Cascadia subduction zone. In comparison, the

Sovanco Transform has not exhibited as much seismic activity. However, the Sovanco Transform seismicity is distributed over a broader area, encompassing the southern Explorer plate from the Nootka Fault westward of the Explorer Ridge. This distribution is likely due to Sovanco's wide fault zone and to increased location error in this part of the study area (Figures 1 and 4). The Mendocino Transform has few SOSUS-recorded earthquakes by comparison, but this lack of seismicity may be an artifact attributable to less-than-optimal SOSUS array coverage for the southern

edge of the JdF plate.

The Explorer and Gorda plates are also very seismically active, producing thousands of SOSUS-recorded earthquakes as well as six $M_w > 6$ (Explorer Plate–Nootka Fault) and three $M_w > 6$ and two $M_w > 7$ (Gorda plate) earthquakes recorded on land-based seismic networks in 1991 and 1992. The 1991 $M_w 7.1$ Gorda plate earthquake is one of the largest earthquakes recorded within the plate in the last 20 years, and its aftershock pattern (including a $M_w 6.6$ event) was a dominant intraplate event. The high seismic levels of these

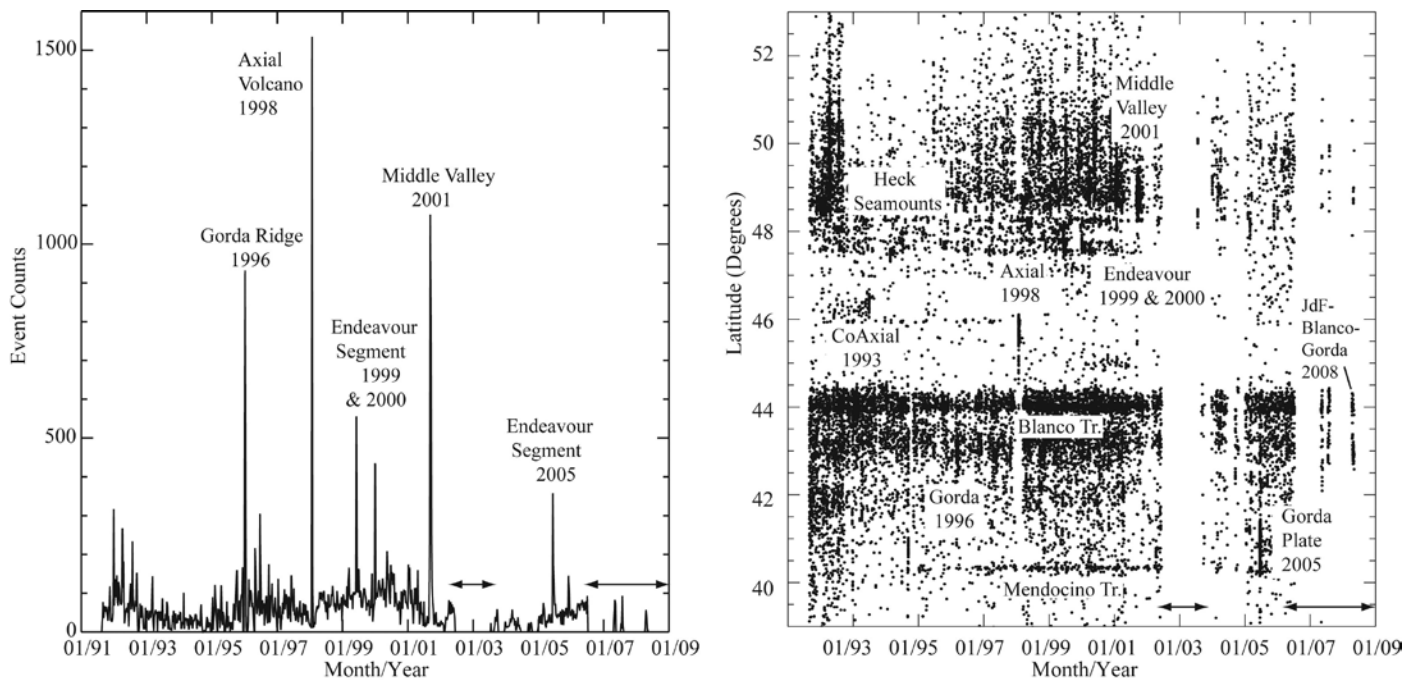


Figure 4. (left) Diagram of total earthquake counts (weekly average) through time for the entire Juan de Fuca plate boundary system. (right) Diagram showing all SOSUS events as a function of latitude through time. The largest periods of activity correspond to volcanic eruptions/seafloor spreading events, which are labeled with event names and dates (Dziak et al., 2007). However, over the long term, the Blanco Transform produces the most earthquakes compared to other Northeast Pacific plate boundaries, with the western transform segment ($\sim 44^\circ\text{N}$) the most seismically active. The relatively high levels of seismicity in late 1991 and early 1992 are due to the Heck Seamount earthquake sequence and Gorda intraplate seismicity preceding the April 1992 Cape Mendocino subduction earthquake (Fox and Dziak, 1999). The 2005 Gorda intraplate earthquake ($M_w 7.2$) along with its aftershocks also stand out as a significant intraplate deformation event. The Mendocino Transform exhibits steady background seismicity at 40.5°N . The variation in background earthquake levels through time is due to changes in the SOSUS arrays available to locate earthquakes, which can influence location error and detection threshold. The time periods with exceptionally low levels of earthquake activity (2002–2003; 2008–2009) are times when SOSUS coastal arrays were disabled (annotated by double arrows). The arrays were also down before and after the 1998 Axial Volcano eruption, identified by the lack of events on the other ridge segments. Very few earthquakes are available through 2010; thus, the diagram only shows data through 2009 to keep the figure resolution high.

microplates are consistent with interpretations that these areas are highly fractured deformation zones rather than true plates (Wilson, 1989; Dziak, 2006). Their increased deformation relative to the central JdF plate is likely due to the young crustal age in these regions and the high deformation rates associated with triple junctions. The Gorda plate internal deformation appears linked to stress release at the subduction zone, where months-long occurrences of SOSUS-recorded earthquakes within the plate ceased when, in April 1992, a M_w 7.2 earthquake occurred at the subduction zone at the coast near the triple junction (Fox and Dziak, 1999). In 2005, another M_w 7.2 occurred within the Gorda plate, further demonstrating the ongoing high deformation rates of this intraplate zone (Chaytor et al., 2005). The Gorda and Explorer Ridges adjacent to these rapidly deforming microplates are themselves also highly seismically active, indicating that the intense state of stress imposed on the microplate may affect deformation rates at the Gorda and Explorer Ridges as well.

The Juan de Fuca intraplate region exhibits very few earthquakes relative to the high earthquake rates at the Gorda and Explorer plates. The two notable exceptions to this observation are the cluster of 50+ earthquakes at 45°N, 128°W and the March 2008 intraplate earthquake swarm centered ~ 70 km north of central Blanco Transform. The 45°N intraplate cluster is unusual in that the events in the cluster occurred over a 20-year interval. This slow, but steady rate of earthquakes implies a very slow intraplate deformation rate.

The March 2008 swarm, on the other hand, is the first true intraplate

earthquake swarm observed in 20 years of SOSUS monitoring. During a 10-day period, more than 600 earthquake epicenters were located and the time history of the earthquakes indicates it was not a typical mainshock-aftershock sequence. The activity was centered on the southern edge of a mid-plate high that rises above the surrounding abyssal sediments. The earthquake activity showed an interesting spatio-temporal progression, beginning in the middle of the plate, moving next to the transform, then manifesting as a seafloor spreading event at the northern Gorda Ridge. The continuity of the swarm across plate boundaries implies that the JdF plate acts as a coherent, rigid plate over distances of hundreds of kilometers. The intraplate swarm likely initiated as a result of stresses induced on the region by transform push forces and a locked subduction interface (Merle et al., 2008).

One of the largest seismic sequences observed on SOSUS occurred in January 1992 along the Heck Seamounts, a volcanic chain extending west from the Endeavour segment of the Juan de Fuca Ridge. The mainshock was a M_w 6.0 strike-slip fault earthquake that produced 840 SOSUS-detected aftershocks that were located along the south side of the seamount chain. The mainshock's focal mechanism and the linear distribution of aftershocks indicate this earthquake sequence was along a previously unidentified right-lateral strike-slip fault paralleling the Heck Seamounts. The earthquakes were interpreted as caused by a zone of shear parallel to, but well south of, the Sovanco Transform that extends to the Cobb Offset along the Juan de Fuca Ridge, reflecting southward reorganization of the Pacific–JdF–North

America triple junction (Dziak, 2006).

The Cascadia subduction zone has long been viewed as aseismic. Few earthquakes (2–5 m_b) have been detected at the interplate interface because the interface is currently locked (Heaton and Hartzel, 1987). Motion on the deeper interface, however, does occur during month-long cycles of slow slip and tremor-like (non-earthquake) seismic events (Rogers and Dragert, 2003). The SOSUS earthquake database seems to support these findings, indicating an aseismic subduction zone to the SOSUS detection level of $m_b \sim 2.5$. However, as noted earlier, the SOSUS arrays are not optimally located for recording earthquakes from the subduction zone; thus, the SOSUS detection threshold for these earthquakes could be on the order of one magnitude higher than for other regions of the JdF plate. Although a concerted effort has been made to identify subduction tremor on the hydrophone records, no tremor events have yet been conclusively found.

Spatio-Temporal Patterns in Northeast Pacific Earthquake Activity

To further quantify these first-order observations, Empirical Orthogonal Functions (EOF; Preisendorfer and Mobley, 1988) were employed to elucidate space-time patterns in the earthquake data and compare earthquake rates and patterns from the various ridge segments and transforms (Figure 5A,B). EOF analysis is a decomposition of a data set in terms of orthogonal basis functions that are objectively determined from the data themselves. Here, the basis functions were found by computing the eigenvectors of the covariance matrix

from the earthquake source information (origin time and location). We found the EOF technique useful in identifying the time and location of earthquake clusters with the largest total number of events in the SOSUS database. Thus, the EOF analysis helped us identify geological features or structures that were the major focus of earthquake activity over the last 20 years.

To calculate the EOF, the earthquake data were separated into 10' x 10' spatial grids, then the mean earthquake count was calculated for that grid over the 20-year time span that the data (green areas in Figure 5A) were collected. The earthquake data are then broken into one-month time bins, and the dominant modes (event clusters) show up as periods of time and locations when the

earthquake counts significantly exceed the mean. Figure 5B shows that four clusters (modes) account for ~ 99% of the variance in the entire SOSUS data set. Figure 5c shows the date the largest event clusters occurred and the total number (amplitude) of the events that month. Interestingly, the earthquake sequences with the largest number of events (dominant modes of variability)

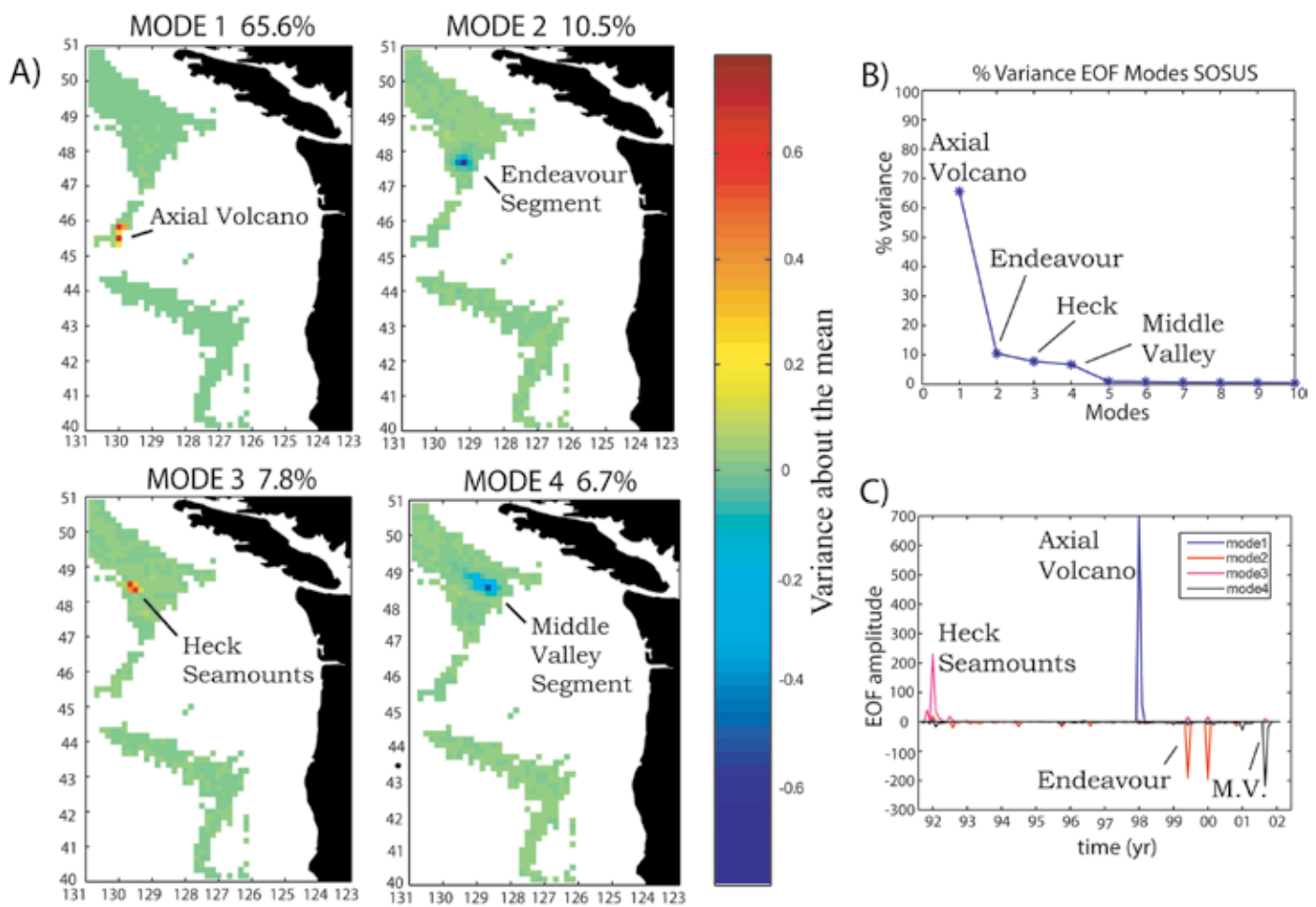


Figure 5. (A) Empirical Orthogonal Function (EOF) analysis of the Northeast Pacific SOSUS catalog produces four distinct event clusters that account for 90.6% of the variability shown in the eigenvalues diagram (B and C). The green values in (A) represent the mean earthquake count (zero variance) within 10' x 10' spatial grids over the 20-year time span of the data. To calculate the EOF, the earthquake data for each 10' x 10' grid is broken into one-month time bins. The dominant modes (event clusters) show up as periods of time and locations when the earthquake counts significantly exceed the mean. (B) This panel shows that four clusters (modes) account for ~ 99% of the variance in the entire SOSUS data set. (C) This panel shows the date the largest event clusters occurred and the total number (amplitude) of the events that month. The January 1998 eruption of Axial Volcano (Dziak and Fox, 1999) is the first mode (65.6%) and dominates the variance within the record. The second mode (10.5%) is the Endeavour segment swarms in June 1999 and January 2000 (Bohnenstiehl et al., 2004), which explains why there are two EOF peaks for this mode in (C). The third mode (7.8%) is due to seismic activity observed along the Heck Seamount Chain in early 1992. The fourth mode of variability (6.7%) describes the spatial and temporal pattern of seismicity rate change associated with the Middle Valley (M.V.) earthquake swarm (Davis et al., 2004).

occur on ridge segments and not on the transform faults. Our EOF analysis of the Northeast Pacific *T*-wave earthquake catalog produces four distinct modes of variability shown in the eigenvalues diagram (Figure 5B,C). The January 1998 eruption of Axial Volcano (Dziak and Fox, 1999) was the first mode (65.6%) and dominates the variance within the entire 20-year catalog as the single largest earthquake sequence. The Endeavor segment swarms in June 1999 and January 2000 (Bohnenstiehl et al., 2004) are the second mode (10.5%), and the third mode (7.8%) was the mainshock-aftershock seismic sequence observed along the Heck Seamount Chain in early 1992 (Dziak, 2006). The fourth mode of variability (6.7%) describes the spatial and temporal pattern of seismicity rate change associated with the Middle Valley earthquake swarm (Davis et al., 2004). No transform clusters stand out in the EOF analysis because no transform earthquake sequence (mainshock-aftershock) had a total number of events that significantly exceeded the 20-year mean event count at that location. Thus ridge-crest event swarms, when they occur, far exceed background earthquake levels as compared to transform event sequences.

Ridge-Crest Seafloor Spreading Events

Making SOSUS available to the civilian research community has fundamentally improved our ability to detect and locate transient mid-ocean ridge (MOR) earthquake activity associated with active submarine volcanoes. Indeed, the use of hydroacoustic methods to detect MOR volcanic activity has met with surprising success, beginning with the first real-time observation of a

lateral dike injection and seafloor eruption episode at the CoAxial segment on the Juan de Fuca Ridge in 1993 (Fox et al., 1995; Dziak et al., 1995). The remote detection of this volcanic episode resulted in several in situ multidisciplinary studies (Baker et al., 1995; Embley et al., 1995) as well as providing clear evidence that microbial communities exist in a subseafloor ecosystem at mid-ocean ridges (e.g., Holden et al., 1998). Four response cruises over the following few months found and sampled three event plumes at CoAxial, in addition to chronic plumes and a still-cooling lava flow. Two other major eruptive episodes have been documented at the northern Gorda Ridge in 1996 (Fox and Dziak, 1998) and Axial Volcano in 1998 (Dziak and Fox, 1999), as well as dike injection/seafloor spreading episodes at the Endeavour segment in 1999 and 2005 (Bohnenstiehl et al., 2004; Hooff et al., 2010). A response cruise was not organized for the 1999 Endeavour swarm because it was viewed as a tectonic episode without a volcanic component. A response cruise did go to the site of the 2005 swarm, but no physical or chemical water-column evidence of a seafloor eruption was found. Later retrieval of in situ instruments documented significant temperature and chemical changes at the Endeavour hydrothermal fields as well as local microearthquake activity likely related to a shallow magma dike intrusion associated with both the 1999 and 2005 swarms. Prolonged, intrusion-style earthquake swarms were also observed at both the Gorda Ridge (Jackson segment) and the Middle Valley segment in 2001, and response cruises were sent to investigate the sites. In both cases, no

seafloor eruptions or event plumes were found, even though the Middle Valley event was an extremely large earthquake swarm (> 14,000 events). Middle Valley has a thick (~ 100 m) sediment cap, and a large negative fluid-pressure change was recorded at an on-axis Ocean Drilling Program drillhole during the swarm, suggesting fluid was entrained, rather than expelled, during the event (Davis et al., 2004).

Because in situ observations have confirmed that only three out of seven SOSUS-detected earthquake swarms were associated with seafloor volcanic eruptions and hydrothermal plume release, all ridge earthquake swarm data were examined in an attempt to identify parameters that could refine the ability to recognize extrusive volcanic activity associated with future earthquake swarms (Dziak et al., 2007). Swarm characteristics such as total and mean number of events, swarm duration, and peak intensity were considered. Two characteristics appear particularly important for distinguishing earthquake swarms associated with eruptions and hydrothermal discharge. The first is the earthquake migration rate, which tracks the down-rift movement of magma. The second is onset time of down-rift earthquake migration, or the time interval between the onset of earthquake activity at the magma source and the time when the dike is injected and begins to propagate down-rift (Dziak et al., 2007). Higher propagation rates and shorter onset times to the beginning of event migration are related to a higher excess magma pressure at the dike source, resulting from a new influx of melt from the mantle (Rubin, 1995; Jaupart and Tait, 1995). Events with these

high-pressure diking characteristics are more likely than others to have manifestations at the seafloor, and probably occur when the shallow-crust magma reservoirs are fed by periodic influxes of melts ascending from a mantle reservoir.

DISCUSSION

Overall, the Northeast Pacific spreading centers exhibit both high levels of continued background seismicity (Explorer and Gorda segments) and long periods of quiescence punctuated by brief periods (days to weeks) of intense (> 1000 events/day) earthquake activity. The Juan de Fuca Ridge from the Cobb Offset to the Blanco Transform is largely aseismic (with the notable exceptions of two brief eruption events) down to the SOSUS ~ 2.5 m_b level of completeness, implying that much of the extension at the ridge occurs through infrequent (decades to centuries) dike intrusion events, or that seafloor spreading at the ridge crest occurs aseismically or at a lower seismic threshold. It is also possible that several of the Juan de Fuca Ridge segments that are currently aseismic do produce intrusion events with thousands of associated earthquakes, but that the eruption cycle is greater than the 20-year SOSUS recording period. In contrast, the Endeavour, Explorer, and Gorda Ridges are highly seismic and produce nearly continuous earthquake activity. In addition to exhibiting constant background seismicity, the Endeavour and Gorda Ridges have also been punctuated by large volcanogenic earthquake swarms. These swarms indicate that the ridge segments may undergo two phases of seafloor spreading, where ridge extension can be accommodated by both

tectonically driven slip on ridge-crest faults and/or magma dike intrusion.

There is a clear overall pattern in the SOSUS seismicity of the JdF plate. The SOSUS seismicity concentrates to the north at the Explorer plate, as well as exhibiting high seismic activity along the adjacent Explorer Ridge and Sovanco Fracture Zone. The same is true for the Gorda plate, where both the intraplate and the adjacent Gorda Ridge segments are very seismically active. Thus, the northern and southern sections of the JdF plate are seismically active and exhibit high relative deformation rates, whereas the central JdF plate and adjacent Juan de Fuca Ridge produce far fewer earthquakes. We interpret this pattern as further evidence that the Explorer and Gorda “plates” are deformation zones structurally independent of the JdF plate, with rapid deformation rates possibly because these zones reflect the broad area of stress induced by the adjacent triple junctions. More interestingly, this structural independence suggests the JdF plate is segmented, which, if true, implies that the downgoing plate at the subduction interface is also segmented. A segmented JdF plate separated into three distinct regions has important implications for rupture behavior during future subduction zone earthquakes, where segment boundaries can act as barriers to rupture propagation (Robinson et al., 2006; Goldfinger et al., 2003). Thus, subduction earthquakes could be limited in size due to these segment boundaries, where each segment rupture would be a $M_w > 8$ earthquake, but not necessarily an all encompassing $M_w 9$ earthquake where the entire zone ruptures in a single event. This interpretation is consistent with

Cascadia subduction zone segmentation models derived from turbidite data (Goldfinger et al., 2003).

In contrast to the megathrust earthquakes that occur at several hundred year intervals, the Cascadia subduction zone has long been viewed as nearly aseismic, exhibiting few background earthquakes. Our 20-year record of SOSUS monitoring also appears to confirm a lack of interplate seismicity along the Cascadia subduction zone; however, this may be due to insufficient SOSUS array coverage of the subduction zone.

The Blanco Transform exhibits the highest levels of nearly continuous earthquake activity and total seismic energy release in the Northeast Pacific Ocean. The Blanco Transform has two clear seismic segments, where the western segment produces an order of magnitude more earthquakes than the eastern segment. The western Blanco is broken into three small strike-slip fault segments separated by large pull-apart basins, whereas the eastern Blanco is essentially one ~ 110 km strike-slip fault (Embley and Wilson, 1992). This continuity results in the eastern Blanco Transform producing fewer, but larger, earthquakes (Dziak et al., 1991). The eastern Blanco Transform is the most consistent producer of the largest earthquakes in the region, with five $M_w > 6$ earthquakes since 1991 (Boetcher and McGuire, 2009). During March 2008, an intense (> 600 events) earthquake swarm occurred 50 km north of the Blanco Transform within the JdF plate (Figure 1; Merle et al., 2008). This intraplate swarm was followed by a progression of three more earthquake swarms that were focused on the central Blanco

Transform, the eastern transform, then the northern Gorda Ridge. This sequence appears to show that strain release can begin within a plate and be transmitted across hundreds of kilometers of the adjacent plate boundary.

The Sovanco Transform exhibits a bookshelf faulting style, with rhombohedron-shaped oblique-slip structures (Cowan et al., 1986). The small individual fault segments therefore produce smaller-magnitude events ($M_w < 6$) than the Blanco. Because the Sovanco is adjacent to the Explorer plate, this transform structure likely reflects the oblique shear and high deformation rates evident in the entire region, which likely explains why the Sovanco exhibits a similar level of earthquake activity compared to the entire Explorer intraplate deformation zone. By comparison, the Mendocino Transform has few SOSUS-recorded earthquakes, but this lack of seismicity is likely due to insufficient SOSUS array coverage for the southern edge of the JdF plate. However, the Mendocino Transform did produce an M_w 7 earthquake in 1994, the largest transform earthquake in the region in the last 20 years. Thus, the Mendocino Transform may very well be a significant source of seismic energy release, but over time periods longer than those covered by this study.

Our EOF analysis of the Juan de Fuca plate system demonstrates the importance of the eruption at Axial Volcano. Not only was it a dominant event, standing out as the largest earthquake swarm yet detected for the entire system, but it also precedes, or may have triggered, increased seismicity along other Juan de Fuca Ridge segments. Figure 4 shows a total count of earthquakes

through time for the entire JdF plate boundary system. In general, there are several peaks in the activity, with Northeast Pacific earthquake maximums during 1991–1992 and from early 1998 to 2002. The peak in earthquake activity observed during 1991 and 1992 is due to the Heck Seamount earthquake sequence and the Gorda intraplate sequence that preceded the April 1992 Cape Mendocino subduction zone earthquake (Fox and Dziak, 1999). The onset of the two-year increase in activity from 1998 to 2002 on all JdF plate boundaries coincides with the 1998 Axial eruption, the largest single earthquake swarm in the last 20 years. This two-to-three-year increase in seismic activity includes notable large earthquake swarms on the Endeavour segment (1999), the Gorda Ridge (2001), and in Middle Valley (2001), as well as a general increase in events along the northern Juan de Fuca Ridge segments and the Blanco Transform (Figure 4, right). It is intriguing to speculate that this may have been a period of heightened stress on all JdF plate boundary faults, and, if true, would be all the more remarkable given the large spatial and tectonic separation of the sites. However, given the changes to the number and location of SOSUS arrays available during the period of this study, it is impossible to unequivocally conclude that such variability in background earthquake levels is not wholly, or in part, an artifact of the hydrophone system. The increased event total during 2005 and 2006 is due to the aftershocks from the 2005 M_w 7.2 Gorda intraplate earthquake, the largest earthquake recorded within the plate in the last 20 years.

CONCLUDING OBSERVATIONS

This 20-year, globally unique earthquake monitoring effort combining military assets and civilian scientific capabilities has greatly improved our understanding of ocean floor volcanic and tectonic processes. The SOSUS data allowed researchers for the first time to establish the time and distance scales of mid-ocean ridge seafloor spreading events, which constitute the fundamental process for creation of Earth's oceanic crust. Use of SOSUS has also led to some of the first incontrovertible evidence for a shallow, subsurface biosphere beneath mid-ocean ridges and provides insight into fault slip processes at transforms and subduction zones. During the period of observation, striking patterns of earthquake activity are immediately obvious. Most of the plate boundaries are characterized by numerous, mostly low-magnitude events. Some boundaries, however, do not appear to be similarly active during the period of study. The most striking of these boundaries is the axis of the Juan de Fuca spreading center and the Cascadia subduction zone. If this aseismic behavior is real, and not just an artifact of a relatively short, 20-year recording period or attributable to the limitations of the SOSUS arrays, then it poses interesting questions about the mechanisms of slip and seismic coupling along these ocean plate interfaces.

Access to SOSUS data has made it possible, for the first time, to observe and acquire quantitative information about deep-ocean volcanic eruption mechanisms and processes. The ability to make such observations is critical because seafloor volcanic eruptions are the most common eruptions on Earth, and they produce physical and

chemical impacts that, over geologic time, influence the global state of the ocean. Submarine volcanic eruptions can produce prodigious quantities of heat as well as volatiles (e.g., CO₂) and elements (e.g., nutrients such as Fe, Ca, and P) that are important to the ocean's macro- and microbiospheres. While the past 20 years of SOSUS monitoring has been successful, it is also clear that continued observations are required if we are to understand recurrence intervals and potential space-time linkages of these ocean plate boundary processes. Now that comprehensive observation systems exist for monitoring surface ocean events (e.g., El Niño and tsunamis), expanding our deep-ocean hydrophone monitoring systems using both cabled arrays and satellite-telemetry buoys is also critical to better understanding the pace and distribution of otherwise unobserved seafloor volcanic and tectonic activity.

ACKNOWLEDGEMENTS

The authors thank the US Navy personnel at the Naval Ocean Processing Facility at Naval Air Station, Whidbey Island, for their generous assistance and support that has allowed the continued flow of SOSUS hydrophone data to our NOAA/OSU labs during the last 20 years. We also give special thanks to J. Peeples, H. Milburn, D. Seem, and E. Bernard for their engineering, computer, and strategic support that allowed this project to become a reality in August 1991. We also very gratefully acknowledge the hard work and unselfish efforts of T.-K. Lau, J. Haxel, M. Fowler, J. Klay, H. Matsumoto, C. Meinig, M. Koehn, A.E. Radford, and J. Graham in developing and maintaining the data acquisition

hardware and analysis software, for data processing, and for helping with the myriad Department of Commerce and Department of Energy security issues we have had throughout the years. The authors are further indebted to S. Merle for graphics production and R. Embley for provocative discussions over the years. The authors also wish to thank M. Tolstoy, E. Hooft and D. Wilson for very helpful reviews that improved the manuscript. The project was supported during 2006–2009 by National Science Foundation grant OCE-0623649. This paper is NOAA/PMEL contribution number 3714. 

REFERENCES

- Baker, E.T., G.J. Massoth, R.A. Feely, R.W. Embley, R.E. Thomson, and B.J. Burd. 1995. Hydrothermal event plumes from the CoAxial seafloor eruption site, Juan de Fuca Ridge. *Geophysical Research Letters* 22(2):147–150, <http://dx.doi.org/10.1029/94GL02403>.
- Boettcher, M.S., and J.J. McGuire. 2009. Scaling relations for seismic cycles on mid-ocean ridge transform faults. *Geophysical Research Letters* 36, L21301, <http://dx.doi.org/10.1029/2009GL040115>.
- Bohnenstiehl, D.R., R.P. Dziak, M. Tolstoy, C. Fox, and M. Fowler. 2004. Temporal and spatial history of the 1999–2000 Endeavour Segment seismic series, Juan de Fuca Ridge. *Geochemistry, Geophysics, Geosystems* 5, Q09003, <http://dx.doi.org/10.1029/2004GC000735>.
- Bohnenstiehl, D.R., M. Tolstoy, R.P. Dziak, C.G. Fox, and D.K. Smith. 2002. Aftershock sequences in the mid-ocean ridge environment: An analysis using hydroacoustic data. *Tectonophysics* 354(1–2):49–70, [http://dx.doi.org/10.1016/S0040-1951\(02\)00289-5](http://dx.doi.org/10.1016/S0040-1951(02)00289-5).
- Braunmiller, J., and J. Nabelek. 2008. Segmentation of the Blanco Transform Fault Zone from earthquake analysis: Complex tectonics of an oceanic transform fault. *Journal of Geophysical Research* 113, B07108, <http://dx.doi.org/10.1029/2007JB005213>.
- Chaytor, J.D., C. Goldfinger, R.P. Dziak, C.G. Fox. 2004. Active deformation of the Gorda plate: Constraining deformation models with new geophysical data. *Geology* 32(4):353–356, <http://dx.doi.org/10.1130/G20178.2>.

- Cowan, D.S., M. Botros, and H.P. Johnson. 1986. Bookshelf tectonics: Rotated crustal blocks within the Sovanco Fracture Zone. *Geophysical Research Letters* 13(190):995–998, <http://dx.doi.org/10.1029/GL013101p00995>.
- Davis, E.E., K. Becker, R. Dziak, J. Cassidy, and K. Wang. 2004. Hydrologic response to a seafloor spreading episode on the Juan de Fuca Ridge. *Nature* 430:335–338, <http://dx.doi.org/10.1038/nature02755>.
- Dziak, R.P. 2006. Explorer deformation zone: Evidence of a large shear zone and reorganization of the Pacific–Juan de Fuca–North American triple junction. *Geology* 34(3):213–216, <http://dx.doi.org/10.1130/G22164.1>.
- Dziak, R.P., and C.G. Fox. 1999. The January 1998 earthquake swarm at Axial Volcano, Juan de Fuca Ridge: Hydroacoustic evidence of seafloor volcanic activity. *Geophysical Research Letters* 26(23):3,429–3,432, <http://dx.doi.org/10.1029/1999GL002332>.
- Dziak, R.P., D.R. Bohnenstiehl, J.P. Cowen, E.T. Baker, K.H. Rubin, J.H. Haxel, and M.J. Fowler. 2007. Rapid dike emplacement leads to eruptions and hydrothermal plume release during seafloor spreading events. *Geology* 35(7):579–582, <http://dx.doi.org/10.1130/G23476A.1>.
- Dziak, R.P., D.R. Bohnenstiehl, H. Matsumoto, C.G. Fox, D.K. Smith, M. Tolstoy, T.-K. Lau, J.H. Haxel, and M.J. Fowler. 2004. P- and T-wave detection thresholds, Pn velocity estimate, and detection of lower mantle and core P-waves on ocean sound channel hydrophones at the Mid-Atlantic Ridge. *Bulletin of the Seismological Society of America* 94:665–677, <http://dx.doi.org/10.1785/0120030156>.
- Dziak, R.P., W.W. Chadwick, C.G. Fox, and R.W. Embley. 2003. Hydrothermal temperature changes at the southern Juan de Fuca Ridge associated with a M_w 6.2 Blanco Transform earthquake. *Geology* 31:119–122, [http://dx.doi.org/10.1130/0091-7613\(2003\)031<0119:HTCATS>2.0.CO;2](http://dx.doi.org/10.1130/0091-7613(2003)031<0119:HTCATS>2.0.CO;2).
- Dziak, R.P., C.G. Fox, and A.E. Schreiner. 1995. The June–July seismo-acoustic event at CoAxial segment, Juan de Fuca Ridge: Evidence for lateral dike injection. *Geophysical Research Letters* 22(2):135–138, <http://dx.doi.org/10.1029/94GL01857>.
- Dziak, R.P., C.G. Fox, and R.W. Embley. 1991. Relationship between the seismicity and geologic structure of the Blanco Transform Fault Zone. *Marine Geophysical Researches* 13:203–208, <http://dx.doi.org/10.1007/BF00369149>.
- Embley, R.W., and E.T. Baker. 1999. Interdisciplinary group explores seafloor eruption with remotely operated vehicle. *Eos, Transactions, American Geophysical Union* 80:213, 219, 222, <http://dx.doi.org/10.1029/99EO00157>.

- Embley, R.W., and D.S. Wilson. 1992. Morphology of the Blanco Transform Fault Zone—NE Pacific: Implications for its tectonic evolution. *Marine Geophysical Researches* 14:25–45, <http://dx.doi.org/10.1007/BF01674064>.
- Embley, R.W., W.W. Chadwick Jr., I.R. Jonasson, D.A. Butterfield, and E.T. Baker. 1995. Initial results of a rapid response to the 1993 CoAxial event: Relationships between hydrothermal and volcanic processes. *Geophysical Research Letters* 22(2):143–146, <http://dx.doi.org/10.1029/94GL02281>.
- Embley, R.W., W.W. Chadwick Jr., D. Stakes, and D. Clague. 1999. 1998 eruption at Axial Volcano: Multibeam anomalies and seafloor observations. *Geophysical Research Letters* 26:3,425–3,428, <http://dx.doi.org/10.1029/1999GL002328>.
- Fox, C.G., and R.P. Dziak. 1998. Hydroacoustic detection of volcanic activity on the Gorda Ridge, February–March 1996. *Deep-Sea Research Part II* 45(12):2,513–2,530, [http://dx.doi.org/10.1016/S0967-0645\(98\)00081-2](http://dx.doi.org/10.1016/S0967-0645(98)00081-2).
- Fox, C.G., and R.P. Dziak. 1999. Internal deformation of Gorda Plate observed by hydroacoustic monitoring. *Journal of Geophysical Research* 104(B8):17,603–17,615, <http://dx.doi.org/10.1029/1999JB900104>.
- Fox, C.G., and S.R. Hammond. 1994. The VENTS Program T-phase project and NOAA's role in ocean environmental research. *Marine Technology Society Journal* 27(4):70–74.
- Fox, C.G., H. Matsumoto, and T.-K. Lau. 2001. Monitoring Pacific Ocean seismicity from an autonomous hydrophone array. *Journal of Geophysical Research* 106:4,183–4,206, <http://dx.doi.org/10.1029/2000JB900404>.
- Fox, C.G., W.E. Radford, R.P. Dziak, T.-K. Lau, H. Matsumoto, and A.E. Schreiner. 1995. Acoustic detection of a seafloor spreading episode on the Juan de Fuca Ridge using military hydrophone arrays. *Geophysical Research Letters* 22(2):131–134, <http://dx.doi.org/10.1029/94GL02059>.
- Goldfinger, C., C.H. Nelson, and J.E. Johnson. 2003. Holocene earthquake records from the Cascadia subduction zone and Northern San Andreas Fault based on dating of offshore turbidites. *Annual Review of Earth and Planetary Sciences* 31:555–577, <http://dx.doi.org/10.1146/annurev.earth.31.100901.141246>.
- Haxel, J.H., R.P. Dziak, W.W. Chadwick, and S. Nooner. 2010. Multi-year relationships between surface deformation and seismicity rates at Axial Volcano. Paper presented at the American Geophysical Union 2010 Fall Meeting, San Francisco, CA, December 13–17, 2010, Abstract # OSC-21C-1521.
- Heaton, T.H., and S.H. Hartzell. 1987. Earthquake hazards on the Cascadia Subduction Zone. *Science* 236:162–168, <http://dx.doi.org/10.1126/science.236.4798.162>.
- Holden, J.F., M. Summit, and J.A. Baross. 1998. Thermophilic and hyperthermophilic microorganisms in 3–30°C hydrothermal fluids following a deep-sea volcanic eruption. *FEMS Microbiology Ecology* 25:33–41, <http://dx.doi.org/10.1111/j.1574-6941.1998.tb00458.x>.
- Hooft, E.E.E., H. Patel, W. Wilcock, K. Becker, D. Butterfield, E. Davis, R. Dziak, K. Inderbitzen, M. Lilley, P. McGill, and others. 2010. A seismic swarm and regional hydrothermal and hydrologic perturbations: The northern Endeavour segment, February 2005. *Geochemistry, Geophysics, Geosystems* 11, Q12015, <http://dx.doi.org/10.1029/2010GC003264>.
- Jaupart, C., and S. Tait. 1995. Dynamics of differentiation in magma reservoirs. *Journal of Geophysical Research* 100(B9):17,615–17,636, <http://dx.doi.org/10.1029/95JB01239>.
- Johnson, H.P., M. Hutnak, R.P. Dziak, C.G. Fox, I. Urcuyo, J.P. Cowen, J. Nabelek, and C. Fisher. 2000. Earthquake-induced changes in a hydrothermal system on the Juan de Fuca mid-ocean ridge. *Nature* 407:174–177, <http://dx.doi.org/10.1038/35025040>.
- Johnson, R., J. Northrop, and R. Epply. 1963. Sources of Pacific T-phases. *Journal of Geophysical Research* 68:4,251–4,261.
- McGuire, J.J., M.S. Boettcher, and T.H. Jordan. 2005. Foreshock sequences and short-term earthquake predictability on East Pacific Rise transform faults. *Nature* 434:457–461, <http://dx.doi.org/10.1038/nature03377>.
- Merle, S.M., R.P. Dziak, R.W. Embley, J.E. Lupton, R.R. Greene, W.W. Chadwick, M. Lilley, D.R. Bohnenstiehl, J. Braunmiller, M. Fowler, and J. Resing. 2008. Preliminary analysis of multibeam, subbottom, and water column data collected from the Juan de Fuca Plate and Gorda Ridge earthquake swarm sites, March–April 2008. *Eos, Transactions, American Geophysical Union* 89(53) Fall Meeting Supplement, Abstract #T23B-2025.
- Nooner, S.L., and W.W. Chadwick Jr. 2009. Volcanic inflation measured in the caldera of Axial Seamount: Implications for magma supply and future eruptions. *Geochemistry, Geophysics, Geosystems* 10, Q02002, <http://dx.doi.org/10.1029/2008GC002315>.
- OOI (Ocean Observatories Initiative). 2006. *Review Report of the NSF Conceptual Design Review Panel for the Ocean Observatories Initiative*. Conducted August 14–17, 2006, at the Monterey Bay Aquarium Research Institute in Moss Landing, CA, 69 pp.
- Preisendorfer, R.W., and C.D. Mobley. 1988. *Principal Component Analysis in Meteorology and Oceanography*. Developments in Atmospheric Science 17. Elsevier, New York, 425 pp.
- Riddihough, R. 1984. Recent movements of the Juan de Fuca Plate system. *Journal of Geophysical Research* 89:6,980–6,994, <http://dx.doi.org/10.1029/JB089iB08p06980>.
- Robinson, D.P., S. Das, and A.B. Watts. 2006. Earthquake rupture stalled by a subducting fracture zone. *Science* 312:1,203–1,205, <http://dx.doi.org/10.1126/science.1125771>.
- Rogers, G., and H. Dragert. 2003. Episodic tremor and slip on the Cascadia subduction zone: The chatter of silent slip. *Science* 300:1,942–1,943, <http://dx.doi.org/10.1126/science.1084783>.
- Rubin, A.M. 1995. Propagation of magma-filled cracks. *Annual Review of Earth and Planetary Sciences* 23:287–336, <http://dx.doi.org/10.1146/annurev.earth.23.050195.001443>.
- Sandwell, D.T., and W.H.F. Smith. 1997. Marine gravity data from Geosat and ERS-1 satellite altimetry. *Journal of Geophysical Research* 102:10,039–10,054, <http://dx.doi.org/10.1029/96JB03223>.
- Slack, P.D., C.G. Fox, and R.P. Dziak. 1999. P wave detection thresholds, Pn velocity estimates, and T wave location uncertainty from oceanic hydrophones. *Journal of Geophysical Research* 104(B6):13,061–13,072, <http://dx.doi.org/10.1029/1999JB900112>.
- Smith, D.K., M. Tolstoy, C.G. Fox, D.R. Bohnenstiehl, H. Matsumoto, and M.J. Fowler. 2002. Hydroacoustic monitoring of seismicity at the slow-spreading Mid-Atlantic Ridge. *Geophysical Research Letters* 29, 1518, <http://dx.doi.org/10.1029/2001GL013912>.
- Teague, W.J., M.J. Carron, and P.J. Hogan. 1990. A comparison between the Generalized Digital Environmental Model and Levitus climatologies. *Journal of Geophysical Research* 95:7,183–7,200, <http://dx.doi.org/10.1029/JC095iC05p07167>.
- Tolstoy, I., and M. Ewing. 1950. The T phase of shallow-focus earthquakes. *Bulletin of the Seismological Society of America* 40:25–51.
- Walker, D.A., and S.R. Hammond. 1998. Historical Gorda Ridge T-phase swarms: Relationships to ridge structure and the tectonic and volcanic state of the ridge during 1964–1966. *Deep-Sea Research Part II* 45(12):2,531–2,545, [http://dx.doi.org/10.1016/S0967-0645\(98\)00082-4](http://dx.doi.org/10.1016/S0967-0645(98)00082-4).
- Wang, K., J. He, and E.E. Davis. 1997. Transform push, oblique subduction resistance, and intra-plate stress of the Juan de Fuca plate. *Journal of Geophysical Research* 102:661–674, <http://dx.doi.org/10.1029/96JB03114>.
- Wilson, D.S. 1989. Deformation of the so-called Gorda Plate. *Journal of Geophysical Research* 94:3,065–3,075, <http://dx.doi.org/10.1029/JB094iB03p03065>.